# Analysis of Atmospheric Energy Transport in ERA40 and Implications for Simple Models of the Mean Tropical Circulation

# Analysis of atmospheric energy transport in ERA40 and implications for simple models of the mean tropical circulation

Matthew E. Peters

Zhiming Kuang *

Chris Walker

Department of Earth and Planetary Sciences

and School of Engineering and Applied Sciences,

Harvard University, Cambridge, MA

*Corresponding author address: Zhiming Kuang, Harvard University, Earth and Planetary Sciences Department, 20 Oxford St., Cambridge, MA 02138.

E-mail: kuang@fas.harvard.edu

Abstract

An analysis of atmospheric energy transport in 22 years (1980-2001) of ERA40 re-analysis is presented. In the analyzed budgets, there is a large cancellation between divergences of dry static and latent energy such that the total energy divergence is positive over all tropical oceanic regions except for the east Pacific cold tongue, consistent with previous studies. The west Pacific and Indian Oceans are characterized by a balance between diabatic sources and mean advective energy export, with a small eddy contribution. However, in the central-eastern Pacific convergence zone, total energy convergence by the mean circulation is balanced by sub-monthly eddies, with a small diabatic source. Decomposing the mean advective tendency into terms due to horizontal and vertical advection shows that the spatial variation in the mean advection is due largely to variations in vertical advection; these variations are further attributed to variations in the vertical profile of the vertical velocity. The eddy energy export, due almost exclusively to eddy moisture export, does not exhibit any significant seasonal variation.

The relationship between the eddies and the mean circulation is examined. Large-scale moisture diffusion is correlated with eddy moisture export on (500 km)$^2$ spatial scales implying that eddy activity preferentially dries narrow convergence zones over wide ones. Eddy moisture export is further linked to the depth of mean convection in large-scale convergence zones with larger eddy export associated with shallower circulations. This suggests a mechanism that could contribute to the observed variation in mean divergence profiles across the northern tropical Pacific whereby sea surface temperature gradients set the width of convergence zones and eddy activity modulates the tropospheric relative humidity and diver-

gence profile. The importance of variations in the vertical profile of the vertical velocity and eddies in closing the energy budget implies that simple models of the mean tropical circulation should include these effects.

# 1. Introduction

The First Law of Thermodynamics places a strong constraint on large-scale atmospheric motions by requiring total column integrated energy divergence to balance surface energy exchange, radiative fluxes, and local storage. When combined with the assumption that moist convection constrains the tropical temperature profile to remain close to a moist adiabat, energy conservation has been used as the basis for theoretical models of the tropical circulation (Neelin and Held 1987; Emanuel et al. 1994; Neelin 1997). However, Back and Bretherton (2006) recently concluded that mean vertical circulations in large regions of the tropics import energy, violating some of the assumptions underlying these theoretical models. It is therefore essential, both for understanding the large-scale circulation and for providing a firm foundation for theoretical models, to obtain the best possible estimates of the atmospheric energy budget.

The atmosphere transports dry static energy (DSE; thermal plus potential energy), latent energy (LE) and kinetic energy. In the Tropics, the divergence of kinetic energy transport is generally small, and the divergence of total energy transport is dominated by a cancellation between the divergences of DSE and LE transport (Trenberth and Stepaniak 2003). A detailed computation of atmospheric moisture transport is therefore an important component of an energy budget computation. Given the importance of moisture in determining the intensity and location of deep convection (Sherwood 1999; Bretherton et al. 2004) and the subsequent coupling with the Hadley and Walker circulations, we will pay close attention to this moisture transport and its interaction with large-scale circulations.

An intriguing aspect of the time-mean tropical circulation is the systematic variation in the structure and depth of the divergent circulation across the Pacific and Atlantic Oceans. Fig. 1 shows a 22 year (1980-2001) climatology of relative humidity and divergence from the Euro-

pean Centre for Medium-Range Weather Forecasts (ERA40) pressure level archive averaged across the northern Intertropical Convergence Zone (ITCZ) from 7.5$^o$N to 10$^o$N. In the western Pacific (50$^o$ - 180$^0$), mean convergence extends from the surface up to 400 hPa while the eastern Pacific ITCZ is characterized by boundary layer convergence below 850 hPa and divergence above associated with a "shallow return flow" above the boundary layer (Zhang et al. 2004). This systematic variation is present in both the annual mean and in the boreal summer-fall when the northern ITCZ is strongest. The middle and upper troposphere in the eastern Pacific is relatively drier than in the western Pacific, suggesting that this drier atmosphere may be linked to the depth of convection. A goal of the present work is to explore the relationship between the depth of the divergent circulation, the relative dryness of the middle troposphere, and the large-scale atmospheric water transport in tropical convergence zones.

Intrusions of dry air into tropical convergence zones have been extensively studied in the west Pacific (Yoneyama and Parsons 1999; Yoneyama 2003; Cau et al. 2005) and east Pacific (Zuidema et al. 2006). These have been shown to inhibit deep convection, both through entraining dry air into updraft plumes (Redelsperger et al. 2002) and through radiatively forced temperature inversions at the base of the dry layer (Mapes and Zuidema 1996). Several studies have shown that these dry intrusions do not result from local subsidence, but rather have been advected from neighboring climatologically dry subsidence regions by an easterly wave passage (Zuidema et al. 2006) or from the subtropical or extra-tropical upper troposphere, associated with developing extra-tropical cyclones and Rossby wave breaking (Yoneyama and Parsons 1999; Yoneyama 2003; Cau et al. 2005). Given the prevalence of these dry layers and their effect on deep convection, it is natural to ask whether they have any effect on the climatology of convergence zones.

To examine these questions, we compute mean circulation and eddy contributions to the atmospheric energy budget using 22 years of data from the ERA40 re-analysis. We pay particular attention to the physical framework and theory outlined in Sec. 2 so that our analysis is applicable to these previous studies. Trenberth and Stepaniak (2003) estimated the mean and eddy contributions to the total energy budget from NCEP-NCAR re-analysis, and Back and Bretherton (2006) estimated the horizontal and vertical contributions to the budget from both NCEP-NCAR and ERA40 re-analysis. However, Back and Bretherton (2006) used daily-averaged pressure-level data on a $2.5^o$ x $2.5^o$ grid and did not apply a mass correction. Given the inaccuracy of energy budgets computed using re-gridded, pressure level data without a mass correction (Trenberth et al. 2002), our analysis methods follow those in Trenberth and Stepaniak (2003), with some additions for the extra horizontal and vertical advection terms (Sec. 3). The first portion of our results can therefore be considered an update of the Trenberth and Stepaniak (2003) calculations with the new ERA40 product. The second portion of our results (Sec. 4) discusses the statistical relationship between moisture transport, the depth of the divergent circulation and with width of ITCZs. Implications for simplified models of the mean tropical circulation are included in Sec. 5.

# 2. Physical Framework and Theory

Frozen moist static energy (FMSE) is the sum of thermal, potential, and latent energy,

$$h = c_p T + gz + L_v q_v - L_f q_i. \tag{1}$$

Here, $T$ is the absolute temperature, $q_v, q_i$ the water vapor and ice mixing ratios, $c_p$ the heat capacity of dry air at a constant pressure, and $L_v, L_f$ the latent heats of vaporization and fusion.

The column integral of $h$ is conserved in moist adiabatic motions except for conversion between thermal and kinetic energy and frozen precipitation that reaches the ground (the last term in (1) corrects for conversion between liquid and solid water). As these two processes are generally small terms in the total energy budget in the tropics, we will neglect them for simplicity in what follows.

The column-integrated FMSE budget is

$$\frac{\partial \tilde{h}}{\partial t} = -\nabla \cdot (\widetilde{\mathbf{u}h}) + Q \tag{2}$$

where $\mathbf{u}$ and $\nabla$ are the horizontal winds and horizontal divergence operator. A tilde represents a mass-weighted vertical integral

$$\tilde{h} = \int_0^{p_s} h \, dp/g,$$

with $p_s$ the surface pressure. The diabatic term $Q$ reduces to the sum of surface heat fluxes and radiative fluxes; notably convective heating and precipitation cancel in the column budget, a chief benefit for considering FMSE instead of dry static energy or latent energy individually. In steady state or for long time means, (2) reduces to a balance between energy flux divergence and diabatic forcing.

By splitting all fields into their time mean and time dependent components, the time mean advective term in (2) can be written as

$$-\overline{\nabla \cdot (\widetilde{\mathbf{u}h})} = -\nabla \cdot (\widetilde{\overline{\mathbf{u}}\overline{h}}) - \overline{\nabla \cdot (\widetilde{\mathbf{u}'h'})} \tag{3}$$

$$-\nabla \cdot (\widetilde{\overline{\mathbf{u}}\overline{h}}) = -(\overline{\mathbf{u}} \cdot \widetilde{\nabla \overline{h}}) - \widetilde{\overline{\omega} \frac{\partial \overline{h}}{\partial p}} \tag{4}$$

with $\omega$ the vertical pressure velocity, and an overbar and prime denoting time mean and time dependent components. In this paper, time mean will refer to a monthly mean with the eddy terms

representing sub-monthly variations. The term on the left-hand side of (3) is the total advection, TADVH, with the terms on the right-hand side the mean and eddy advection, MADVH and EADVH, respectively. In (4), the terms on the right hand-side will be referred to as HADVH and VADVH, the horizontal and vertical advection. To the extent that kinetic energy transport divergence is small, these terms represent the total atmospheric energy transport divergence.

In analogy with the temperature equation, some theoretical models linearize (2) by dropping the EADVH and HADVH terms and assuming the dominant balance is between energy export due to vertical advection and positive diabatic forcing (Neelin and Held 1987; Bretherton and Sobel 2002). If the system is reduced to one vertical degree of freedom in the divergence as in the Quasi-Equilibrium Tropical Circulation Model (QTCM; Neelin and Zeng 2000), then $\overline{\omega}(\mathbf{x}, p) = \overline{w}(\mathbf{x})\Omega(p)$ and VADVH becomes

$$\widetilde{\overline{\omega}\frac{\partial \overline{h}}{\partial p}} = M\overline{w}(\mathbf{x})$$

$$M = \widetilde{\Omega(p)\frac{\partial \overline{h}}{\partial p}},$$

where $\Omega(p)$ is the vertical structure function for $\overline{\omega}$. $M$ is called the gross moist stability and it gives the atmosphere's efficiency at exporting FMSE due to vertical motions. The vertical advection term in the temperature equation can be similarly reduced and written as

$$\widetilde{\overline{\omega}\frac{\partial \overline{s}}{\partial p}} = M_s\overline{w}(\mathbf{x}),$$

with $M_s$ defined analogously to $M$ for the dry static energy $s = c_pT + gz$.

Typical values of the moist stability ratio $\alpha = M/M_s$ are between -0.5 and 0.5, with the exact value dependent on both the shape of $\Omega$ and the vertical profiles of $\overline{h}$ and $\overline{s}$. Deeper convection with a top heavy $\Omega$ profile like those found in the western Pacific give positive values of $\alpha$, while shallower convection like that found in the eastern Pacific ITCZ will give negative values of $\alpha$ (Back and Bretherton 2006).

Bretherton et al. (2006) compared the two-dimensional Walker circulation model in Peters and Bretherton (2005) with a cloud-resolving model (CRM) configured in an analogous setup. To account for changes in the vertical structure of $\omega$ in the CRM and to include the horizontal advection and eddy terms, they defined a generalized moist stability ratio

$$\alpha_{CRM} = \frac{\text{MADVH} + \text{EADVH}}{\text{VADVS}} = \frac{\text{TADVH}}{\text{VADVS}}. \tag{5}$$

In both the CRM and in the simplified model, the size of the convecting region is proportional to $\alpha$ and the strength of the circulation proportional to $1/\alpha$. However, there were some important differences between the CRM and simple model, most notably the lack of a single baroclinic mode structure and large EADVH term in the CRM. In one of the CRM simulations (the narrow domain case), eddies drove the energy export from convecting regions against energy import by the mean circulation (EADVH $< 0$, MADVH $> 0$). However, the eddies in the CRM were due to a standing gravity wave, an artifact of the quasi-two dimensional geometry. It is an open question whether an analogous processes is important in the real Tropics, and whether mean tropical circulations may actually import energy into convecting regions.

To examine the effect of direct sea surface temperature forcing on low level convergence in the single mode framework, Sobel and Neelin (2006) added a prognostic boundary layer and coupled it to the QTCM's baroclinic mode. They also added a large-scale moisture diffusion to represent the effect of unmodeled eddies, and found that the strength of the ITCZ was strongly dependent on the strength of the diffusion. As in the narrow domain case in Bretherton et al. (2006), this moisture diffusion dominated the energy export out of the ITCZ against a mean circulation energy import.

All of these studies rely on interpretation of the effective moist static stability ratio $\alpha$ for predicting changes in the intensity and width of convergence zones. We examine the validity

of these model assumptions and the relationships between $\alpha$ and the width and strength of convergence zones in what follows.

# 3. Data and analysis methods

*a. Data*

We use 22 years (1980-2001) of archived output from the European Centre for Medium-Range Weather Forecasts (ERA40) re-analysis, a period when satellite data are available and assimilated into the re-analysis product (Uppala and Coauthors 2005). The model re-analysis is run on a reduced Gaussian grid with triangular spectral truncation at wavenumber 159, and 60 vertical levels. Full resolution dynamical fields are archived every six hours at 00Z, 06Z, 12Z and 18Z in spectral space, with specific humidity, cloud water and cloud ice archived in grid point space.

At each six hour output, we spectrally transformed the scalar vorticity, divergence, temperature and surface pressure to grid point space, interpolated them along with the moisture fields to the corresponding regular Gaussian grid (160 latitude by 320 longitude), and computed the horizontal vector winds from the vorticity and divergence. In the calculations, all horizontal derivatives (divergences, gradients, Laplacians) are performed in spectral space at the full regular Gaussian resolution. We also used a monthly climatology of accumulated total surface precipitation (the sum of large-scale and convective precipitation) from 1980-1999.

Despite significant uncertainties in the represented hydrological cycle, the ERA40 dataset is arguably the most reliable long-term data source for our purposes. See Cau et al. (2005), Sudradjat et al. (2005), Trenberth et al. (2005), and Uppala and Coauthors (2005) for comparisons

of ERA40 data with independent datasets and earlier re-analysis products. Of particular note is the improved skill in representing the effect of mesoscale dry intrusions with horizontal scale of several hundred km (Yoneyama and Parsons 1999) in the deep tropics as compared to earlier re-analyses (Cau et al. 2005).

*b. Analysis methods*

From the six hourly archived data, we computed all of the budget terms in (3) and (4). The computation of TADVH follows the procedure outlined in Trenberth and Stepaniak (2003). For each six-hour output, we integrated the hydrostatic equation to give the geopotential using the archived temperature and surface pressure, formed the product $\mathbf{u}h$, evaluated the vertical integral $\int_0^{p_s} \mathbf{u}h\, dp/g$, took the divergence, and averaged the six-hour divergences into monthly means to give an uncorrected estimate of TADVH. We then applied the column mass correction detailed in Trenberth et al. (2001) to the monthly mean horizontal winds and to the estimated TADVH to yield the final, mass-corrected TADVH. The results are insensitive to whether the mass correction is applied to individual six-hour outputs or to monthly means. In order to validate our analysis method, we also carried out the analysis with ten years (1990-1999) of NCEP-NCAR re-analysis (Kalnay and Coauthors 1996) and compared the results with those computed by Trenberth and Stepaniak (2003, downloaded from `www.cgd.ucar.edu/cas/catalog/newbudgets`). Our calculation with NCEP-NCAR re-analysis matches these results very closely.

MADVH was computed with the monthly mean FMSE, surface pressure, and mass-corrected horizontal winds. EADVH was then computed as the difference between TADVH and MADVH, using (3). In computing HADVH, care must be taken as the horizontal gradient in (4) is on constant pressure surfaces, while ERA40 uses a hybrid vertical coordinate, $\eta$. Pressure in the model

as a function of height is defined to be $p = a + bp_s$ where $a$ and $b$ are vertically varying functions. We may then compute

$$\nabla_p \overline{h} = \nabla_\eta \overline{h} + \frac{\partial \overline{h}}{\partial \eta} \nabla_p \eta = \nabla_\eta \overline{h} - b \frac{\partial \overline{h}}{\partial \eta} \frac{\nabla \overline{p}_s}{a' + b' \overline{p}_s}$$

where $a' = \partial a / \partial \eta$ and similarly for $b'$. Using this relation, HADVH was computed with the monthly mean mass corrected winds, surface pressure,and $\overline{h}$ so that VADVH can be computed as the difference between MADVH and HADVH. We also make use of the monthly mean vertical pressure velocity for additional diagnostics. As a function of model level, it was computed as

$$\overline{\omega}(\eta) = b \overline{\mathbf{u}} \cdot \nabla \overline{p_s} - \int_0^\eta \overline{\mathbf{u}} \cdot \nabla \overline{p_s} \, db - \int_0^{p(\eta)} \overline{\delta} \, dp$$

where the gradients are taken on constant $\eta$ surfaces and $\overline{\delta}$ represents the horizontal divergence.

As a final note, we also computed the column integrated divergence of kinetic energy, and like previous work (Trenberth and Stepaniak 2003) found its contribution to the total energy budget to be small in the Tropics. As a result, we have excluded it from the analysis for simplicity.

# 4. Results

*a. FMSE budget*

Fig. 2 shows the advective terms in (3), re-gridded to a standard T63 Gaussian grid for plotting purposes (96 latitude by 192 longitude). This eliminates small scale detail in the plots and focuses attention on the large-scale patterns. The total advection, TADVH, shows large-scale energy export from nearly all tropical oceanic regions, except for the cold tongue region in the eastern Pacific, matching quite closely in pattern to that computed in Trenberth and Stepaniak

(2003). The magnitude of TADVH is also similar, with differences generally less than 25 W $m^{-2}$ . However, the magnitude differences between the re-analyses are patterned, with larger ERA40 energy export from most tropical locations except for the tropical Pacific between 150E and 200E where ERA40 energy export is less than in the NCEP-NCAR re-analysis (not shown).

The partitioning between mean circulation and eddy contributions to TADVH is significantly different in ERA40 than in NCEP-NCAR, with large eddy contributions (20-40 W $m^{-2}$) to the total energy export in the central and eastern Pacific ITCZ and south Pacific convergence zone (SPCZ). In fact, in the central and eastern ITCZ, FMSE export is driven by the eddies as the mean circulation imports FMSE, in contrast to budget estimates from NCEP-NCAR re-analysis and the pressure level, $2.5^o$ re-gridded ERA40 archive (Trenberth and Stepaniak 2003; Back and Bretherton 2006). The importance of eddies in exporting energy from tropical convergence zones should be incorporated into simple theoretical models of the tropical circulation. It implies that the mean circulation exhibits a form of moist static instability (Back and Bretherton 2006) where an increase in moist static energy column sources (surface or radiative fluxes) cannot be balanced by a stronger mean circulation as assumed in uni-modal models.

The near cancellation of MADVH with EADVH in the central and eastern Pacific ITCZ implies that the diabatic term in (2) must also be small. However, the radiative and surface fluxes in the re-analysis are subject to considerable uncertainties. While ERA40 clear-sky radiative fluxes compare well with independent satellite data (Allan et al. 2004), Uppala and Coauthors (2005) report that there is a 7 W $m^{-2}$ imbalance in the top of atmosphere all sky radiation budget, most likely due to over-reflective model cirrus clouds. These biases in the radiation budget, coupled with potential biases in the surface fluxes, may be reflected in the computed budgets.

The difference from previous estimates could be due to a combination of factors including increased spatial and vertical resolution necessary to capture the fine detail of dry intrusions and improved physical parameterizations and data assimilation (Cau et al. 2005). To isolate the effect of increased horizontal resolution, we first truncated all fields to T42 and re-ran the analysis for 1999. Increased horizontal accounts a 10-30 W $m^{-2}$ difference between EADVH computed with the full resolution data truncated to T85 and the T42 calculation, with the differences acting to increase the magnitude of EADVH in the higher resolution data. The mass correction, while large over portions of the tropics ($> 100$ W $m^{-2}$), is applied to the monthly mean winds and so does not modify EADVH.

We speculate that a likely source of the NCEP-ERA discrepancy is the difference in their cumulus parameterizations. The NCEP reanalysis uses the simplified Arakawa-Schubert scheme (Grell 1993; Pan and Wu 1995), which parameterizes deep convection as a single non-entraining cloud and bases its closure directly on CAPE. On the other hand, the ERA40 convective scheme is based on a bulk entraining/detraining plume model (Tiedtke 1989) which is more responsive to moisture variations in the free troposphere and less prone to total consumption of CAPE. Such differences may be particularly consequential in the re-analyses in the east/central Pacific ITCZ, a region with no sounding data to assimilate (see Fig. 2 of Uppala and Coauthors (2005)).

As discussed in the introduction, dry intrusions into the tropics are due to a combination of tropical and extra-tropical processes. Both appear to contribute to EADVH. Correlations of four times daily time series of EADVH during September in the central Pacific ITCZ with spatially varying time series of OLR and 850 hPa winds suggest that organized tropical convection is at least partly responsible for variations in EADVH. However, an initial attempt to correlate EADVH and wave activity through a spectrally filtered OLR time series was less successful.

By simultaneously animating maps of time varying EADVH and other physical fields, it is clear that extra-tropical influences also contribute to the eddy export.

Waugh and Polvani (2000) computed a climatology of Rossby wave breaking in the deep tropics (10S and 10N) and found that these events occurred almost exclusively during boreal winter (Nov-Feb) and over the central and eastern Pacific (200E-280E) and Atlantic Oceans. Thus, if wave breaking in the deep tropics is the dominant physical mechanism producing EADVH, then EADVH should exhibit a strong seasonal cycle. As Fig. 3 shows, EADVH in the deep tropics does not exhibit a seasonal cycle, implying that other physical processes and/or wave breaking in the subtropics (Postel and Hitchman 1999) are also important.

The breakdown of MADVH into vertical and horizontal components is shown in Fig. 4. As the temperature is nearly horizontally uniform in the tropics, HADVH is dominated by horizontal moisture advection and constitutes a FMSE sink over most tropical oceanic regions (10-50 W $m^{-2}$), except for the eastern Pacific cold tongue where horizontal moist advection increases column FMSE. VADVH is highly spatially variable, with large column sources of FMSE in large-scale subsidence regions and in the eastern Pacific ITCZ where VADVH exceeds 50 W $m^{-2}$. In the western Pacific and Indian Oceans, VADVH contributes a relatively small FMSE export (less than 30 W $m^{-2}$). The spatial variations of VADVH and HADVH are broadly consistent with the energy budgets in Back and Bretherton (2006).

To further illustrate the balance in the northern ITCZ and highlight the differences between the western and eastern Pacific, Fig. 5 shows the various budget terms averaged from 7N-10N over the Pacific. TADVH is negative over the entire region, although it is nearly zero between 220E and 240E. Between 200E and 240E, horizontal dry advection and eddy moisture export are equally important in balancing FMSE import due to vertical motions (VADVH). Over the

western Pacific, the eddy contribution to FMSE export is much smaller, with most of the energy export carried by the mean circulation.

*b. Eddy export as large-scale moisture diffusion?*

Deep convection is strongly tied to atmospheric precipitable water across a broad range of time-scales from daily to monthly (Bretherton et al. 2004), so strongly precipitating regions are wetter than neighboring subsidence regions. The eddy FMSE export in Fig. 2 is due almost entirely to eddy moisture export (not shown), is confined to convergence zones, and outside of the SPCZ is largest where the convergence zone is narrowest. As narrow ITCZs are more susceptible to dry intrusions, this suggests that EADVH may be idealized as a large-scale moisture diffusion, or as a diffusion on the width of ITCZs. To explore this possibility, Fig. 6 shows the Laplacian of total precipitable water ($\nabla^2 \tilde{q}$), block averaged into 4x4 blocks to remove the small-scale noise (as $\nabla^2 \tilde{q}$ is large in regions of steep topography, spectral truncation causes large ringing effects). Outside of the SPCZ, the moisture diffusion is broadly consistent and correlated with EADVH at this scale ($r = 0.72$ using all oceanic points $20^o$S-$20^o$N), although the correlation decreases at smaller scales ($r = 0.46$ for 2x2 block averages).

In order to idealize EADVH as moisture diffusion in a predictive setting (Sobel and Neelin 2006), it is important to understand how the diffusivity varies with ocean basin, seasonality and climatic regime. To compute the implied diffusivity, we regressed monthly mean time series of EADVH onto time series of the Laplacian of precipitable water. The diffusivity over the Atlantic ocean is approximately constant with season, with values of 8-12 x $10^4$ m$^2$ s$^{-1}$ (Fig. 7). Over the central and eastern Pacific, the implied diffusivity exhibits a pronounced seasonal cycle, with larger values found during the winter hemisphere. This implies that a parameterization of

EADVH as moisture diffusion, perhaps augmented with a simple representation of changes in the diffusivity, may be useful in simple models.

*c. Relationship between eddies and depth of the mean circulation*

Eddy export of moisture represents a systematic drying effect on convergence zones, and as dry intrusions into the tropics are known to play a significant role in limiting deep convection, it is natural to ask whether there is any relationship between the amount of eddy moisture export and the depth of the mean circulation in convergence zones. To quantify the depth of the mean convection, we have computed the monthly mean pressure velocity $\overline{\omega}$ and found the height at which $\overline{\omega}$ is a minimum. Top heavy $\overline{\omega}$ where the mean circulation is deeper will be characterized by higher levels of minimum $\overline{\omega}$ than shallower circulations. As Fig. 8 shows, this metric is successful in separating bottom heavy convergence zones from top heavy ones, with the mean level of minimum $\overline{\omega}$ in the central and eastern Pacific typically in the lower troposphere near 850 hPa, and the level of minimum $\overline{\omega}$ in the western Pacific and Indian Oceans above 500 hPa.

To look for relationships between eddy activity, mean moisture export, and $\overline{\omega}$, we proceeded as follows. Monthly mean data were block averaged into 2x2 blocks and separated into the oceanic regions shown in Fig. 8. All convecting boxes in each region (defined as those with monthly mean precipitation larger than 6 mm day$^{-1}$) were binned by HADVH+EADVH and the level of minimum $\overline{\omega}$ to produce the joint probability distribution functions (PDFs) in Fig. 9. In all oceanic regions, decreased moisture export is accompanied by deeper convection. Plots of HADVH or EADVH individually versus the level of minimum $\overline{\omega}$ are very similar to Fig. 9 implying that drying by both the mean horizontal advection and the eddies are linked to shallower $\omega$ profiles.

Fig. 9 points to a fundamental coupling between convection and its large scale environment. If the large scale environment is systematically moistened or dried by eddy activity or mean horizontal advection, this moisture variation is reflected in variations in the depth of the convection. This result also has an interesting interpretation from an energy balance standpoint. Since TADVH must balance surface and radiative fluxes, a decrease in HADVH or EADVH must be associated with an increase in VADVH, if the diabatic fluxes are fixed. Given the the $\overline{\omega}$ dominance in modulating changes in VADVH (Sec. 4d), increased energy export by HADVH or EADVH must correspond to a shallower circulation.

*d. Relation to theoretical results*

As discussed in Sec. 2, the interpretation of uni-modal models relies heavily on column energy budget constraints. It is therefore important to test the extent to which these models are consistent with the diagnosed budget. Since VADVH is a significant part of MADVH, it is of interest to know whether changes in $\omega$, $h$, or both are causing changes in VADVH. Despite the fact that uni-modal models fix the $\omega$ profile, and that $\omega$ systematically varies across the Pacific ITCZ, these models may still be consistent with the diagnosed FMSE budget if changes in VADVH are due mainly to changes in $h$. To isolate the effect of variations in $\omega$, we recomputed VADVH while fixing the $h$ profile as follows. For each monthly-mean, we computed the mean FMSE profile, $\hat{h}$, in all convecting grid boxes between 20$^o$S and 20$^o$N (defined to be points where the monthly averaged precipitation is larger than 6 mm day$^{-1}$). Using $\hat{h}$ and the spatially varying, monthly mean mass-corrected horizontal winds $\overline{\mathbf{u}}$, we computed

$$\hat{\text{VADVH}} = -\nabla \cdot (\widetilde{\overline{\mathbf{u}}\hat{h}}).$$

As $\nabla\hat{h} = 0$, this is equal to

$$\text{VADVH}\hat{\text{H}} = -\nabla \cdot (\widetilde{\overline{\mathbf{u}}\hat{h}}) = -\hat{h}\widetilde{\nabla \cdot \overline{\mathbf{u}}} = -\widetilde{\overline{\omega}\frac{\partial\hat{h}}{\partial p}}$$

by integration by parts. The difference between VADVH and VADV$\hat{\text{H}}$ is therefore due only to changes in $\overline{h}$ and co-varying changes in $\overline{\omega}$ and $\overline{h}$. As Fig. 10 shows, VADV$\hat{\text{H}}$ matches VADVH very closely in all tropical convergence zones, with the difference everywhere less than 30 W m$^{-2}$, and in many cases less than 10 W m$^{-2}$. Therefore, changes in VADVH are mainly due to changes in $\overline{\omega}$ instead of $\overline{h}$ as assumed in uni-modal models.

Since the computed budgets are incompatible with the assumptions underlying uni-modal models, one may now ask whether they are consistent with the general framework developed in Bretherton et al. (2006). Fig. 11 shows that $\alpha_{CRM}$ does vary systematically across the Pacific ITCZ, with smaller values in the central and eastern Pacific than the rest of the tropical convergence zones, consistent with this study's finding that smaller $\alpha_{CRM}$ is tied to a narrower convergence zone. However, there are important differences between the arguments in Bretherton et al. as applied to the Walker circulation and the mechanism hypothesized here as applied to the Hadley circulation. In the Walker circulation, sea surface temperature gradients (and therefore their effect on low level convergence) are small, so the width of the convergence zone is free to vary. In this case, the hypothesis in Bretherton et al. whereby radiative cooling and eddy fluxes modify $\overline{h}$, $\alpha_{CRM}$ and therefore the size of the convecting region may be valid. In the Hadley circulation, sharp meridional sea surface temperature gradients and other large-scale dynamical constraints fix the width of the ITCZ. Given this ITCZ width, eddies, by acting as a large-scale diffusion, systematically dry the atmosphere, limit the depth of convection, and modify the $\overline{\omega}$ profile. This in turn sets the effective moist stability, $\alpha_{CRM}$.

# 5. Discussion and conclusion

This paper has explored the connections between large-scale moisture and energy transport and the time-mean structure of the divergent circulation in tropical convergence zones. We have shown that in the central and eastern Pacific ITCZ, sub-monthly eddies export a significant amount of latent energy while the mean circulation imports energy in a form of gross moist instability. In the western Pacific and Indian Oceans the eddy contribution is small, and energy export by the mean circulation balances diabatic sources. Other than the importance of the eddy term which we argue has important implications for simple models of the mean tropical circulation, our results are largely consistent with the diagnostics in Back and Bretherton (2006). We attribute the difference in the calculation results to our analysis technique that takes advantage of the full resolution model data and incorporates a mass correction.

Eddy moisture export is further correlated with the Laplacian of precipitable water, implying that eddies act as a large-scale moisture diffusion. This moisture diffusion is related to the vertical velocity profile in all convergence zones, with more moisture export associated with shallower mean circulations.

Taken together, these results suggest a mechanism that may contribute to the systematic variation in both the vertical velocity and relative humidity profiles across the Pacific. Sea surface temperature gradients force low-level convergence and set an initial width for ITCZs. The eddies' systematic drying of narrower ITCZs over wider ones limits the tropospheric moisture available for deep convection and results in a shallower mean circulation. From an energy balance standpoint, increased eddy energy export must be balanced by a decreased mean circulation export. As variations in the mean export are due mainly to variations in vertical advection and variations in vertical advection are due to those in the vertical profile of $\omega$, decreases in the

mean export are tied to shallower circulations. In addition, this mechanism also suggests that wider ITCZs are more effective at moistening the middle and upper troposphere than narrow ITCZs.

This energy budget argument is similar in spirit to the interpretation of intermediate complexity models based on one or two vertical modes in that the energy budget is used to constrain the mean circulation. While current uni-mode models assume a fixed vertical profile for $\omega$, we have shown that the vertical velocity profile and moisture co-vary spatially, and that variations in the vertical velocity profile of $\omega$ are crucial for closing the energy budget. An interesting question for future work is to what extent energy budget arguments based on one mode can be generalized to include these effects.

Nolan et al. (2007) have recently put forward a simple model to interpret the shallow circulation in the central and eastern Pacific as a large-scale sea breeze, where sharp meridional sea surface temperature gradients create a pressure reversal above the boundary layer top and mid-upper tropospheric moisture modulates the strength of the shallow circulation. The mechanism outlined here, on the other hand, attempts to tie the shallowness of the circulation to the sharpness of the SST gradient through eddy drying of the troposphere. Further studies, for example with numerical simulations, are needed to examine these proposed mechanisms in more detail to determine their relative importance.

*Acknowledgments*.

This work was supported by a Harvard startup grant. The 2.5 degree pressure level ERA40 data was downloaded from ECMWF's webpage. Full resolution ERA40 and NCEP/NCAR reanalysis products were provided by the Data Support Section at NCAR. The NCAR software

package *Spherepack* was used extensively in this work. Three anonymous reviewers provided comments that led to significant improvements from an earlier draft.

# References


Allan, R. P., M. A. Pamment, and A. Slingo, 2004: Simulation of the earth's radiation budget by the European Centre for Medium-Range Weather Forecasts 40-year Reanalysis (ERA40). *J. Geophys. Res.*, **109**, D18 107, doi: 1029/2004JD004 816.

Back, L. E. and C. S. Bretherton, 2006: Geographic variability in the export of moist static energy and vertical motion profiles in the Tropical Pacific. *Geophys. Res. Letts.*, **33**, L17 810, doi:10.1029/2006GL026 672.

Bretherton, C. S., P. N. Blossey, and M. E. Peters, 2006: Interpretation of simple and cloud-resolving simulations of moist convection-radiation interaction with a mock-Walker circulation. *Theor. Comp. Fluid Dyn.*, doi:10.1007/s00 162–006–0029–7.

Bretherton, C. S., M. E. Peters, and L. E. Back, 2004: Relationships between water vapor path and precipitation over the tropical oceans. *J. Climate*, **17**, 1517–1528.

Bretherton, C. S. and A. H. Sobel, 2002: A simple model of a convectively coupled Walker circulation using the weak temperature gradient approximation. *J. Climate*, **15**, 2907–2920.

Cau, P., J. Methven, and B. Hoskins, 2005: Representation of dry tropical layers and their origins in ERA-40 data. *J. Geophys. Res.*, **110**, D06 110, dio:10.1029/2004JD004 928.

Emanuel, K. A., J. D. Neelin, and C. S. Bretherton, 1994: On large-scale circulations in convecting atmospheres. *Quart. J. Roy. Meteor. Soc.*, **120**, 1111–1143.

Grell, A. G., 1993: Prognostic evaluation of assumptions used by cumulus parameterizations. *Mon. Wea. Rev.*, **121**, 764–787.

Kalnay, E. and Coauthors, 1996: The NCEP/NCAR 40-year re-analysis project. *Bul. Amer. Met. Soc.*, **77**, 437–471.

Mapes, B. E. and P. Zuidema, 1996: Radiative-dynamical consequences of dry tongues in the tropical troposphere. *J. Atmos. Sci.*, **53**, 620–638.

Neelin, J. D., 1997: Implications of convective quasi-equilibria for the large-scale flow. *The physics and parameterization of moist convection*, Kluwer Academic Publishers, Dordrecht, 413–446.

Neelin, J. D. and I. M. Held, 1987: Modeling tropical convergence based on the moist static energy budget. *Mon. Wea. Rev.*, **115**, 3–12.

Neelin, J. D. and N. Zeng, 2000: The first quasi-equilibrium tropical circulation model—formulation. *J. Atmos. Sci.*, **57**, 1741–1766.

Nolan, D. S., C. Zhang, and S.-H. Chen, 2007: Dynamics of the shallow circulation around intertropical convergence zones. *J. Atmos. Sci.*, in press.

Pan, H. L. and W. S. Wu, 1995: Implementing a mass flux convection parameterization package for the NMC medium-range forecast model. *NMC office note*, No 409, 40pp. [Available from NCEP, 5200 Auth Road, Washington, DC 20 233].

Peters, M. E. and C. S. Bretherton, 2005: A simplified model of the Walker circulation with an interactive ocean mixed layer and cloud-radiative feedbacks. *J. Climate*, **18**, 4216–4234.

Postel, G. A. and M. H. Hitchman, 1999: A climatology of Rossby wave breaking along the subtropical tropopause. *J. Atmos. Sci.*, **56**, 359–373.

Redelsperger, J.-L., D. B. Parsons, and F. Guichard, 2002: Recovery processes and factors limiting cloud-top height following the arrival of a dry intrusion observed during TOGA-COARE. *J. Atmos. Sci.*, **59**, 2438–2457.

Sherwood, S. C., 1999: Convective precursors and predictability in the tropical west Pacific. *Mon. Wea. Rev.*, **127**, 2977–2991.

Sobel, A. H. and D. J. Neelin, 2006: The boundary layer contribution to intertropical convergence zones in the quasi-equilibrium tropical circulation model framework. *Theor. Comp. Fluid Dyn.*, **20**, 323–350.

Sudradjat, A., R. R. Ferraro, and M. Fiorino, 2005: A comparison of total precipitable water between reanalyes and NVAP. *J. Climate*, **18**, 1790–1807.

Tiedtke, M., 1989: A comprehensive mass flux scheme for cumulus parameterization in large-scale models. *Mon. Wea. Rev.*, **117**, 1779–1800.

Trenberth, K. E., J. M. Caron, and D. P. Stepaniak, 2001: The atmospheric energy budget and implications for surface fluxes and ocean heat transports. *Climate Dyn.*, **17**, 259–276.

Trenberth, K. E., J. Fasullo, and L. Smith, 2005: Trends and variability in column-integrated atmospheric water vapor. *Climate Dyn.*, **24**, 741–758.

Trenberth, K. E. and D. P. Stepaniak, 2003: Seamless poleward atmospheric energy transports and implications for the Hadley circulation. *J. Climate*, **16**, 3706–3722.

Trenberth, K. E., D. P. Stepaniak, and J. M. Caron, 2002: Accuracy of atmospheric energy budgets from analyses. *J. Climate*, **15**, 3343–3360.

Uppala, S. M. and Coauthors, 2005: The ERA-40 re-analysis. *Quart. J. Roy. Meteor. Soc.*, **131**, 2961–3012.

Waugh, D. W. and L. M. Polvani, 2000: Climatology of intrusions into the tropical upper troposphere. *Geophys. Res. Letts.*, **27**, 3857–3860.

Yoneyama, K., 2003: Moisture variability over the tropical western Pacific ocean. *J. Meteor. Soc. Japan*, **81**, 317–337.

Yoneyama, K. and D. B. Parsons, 1999: A proposed mechanism for the intrusion of dry air into the tropical western Pacific region. *J. Atmos. Sci.*, **56**, 1524–1546.

Zhang, C., M. McGauley, and N. A. Bond, 2004: Shallow meridional circulation in the tropical eastern Pacific. *J. Climate*, **17**, 133–139.

Zuidema, P., B. Mapes, J. Lin, and C. Fairall, 2006: The interaction of clouds and dry air in the eastern tropical Pacific. *J. Climate*, **19**, 4531–4544.

# List of Figures

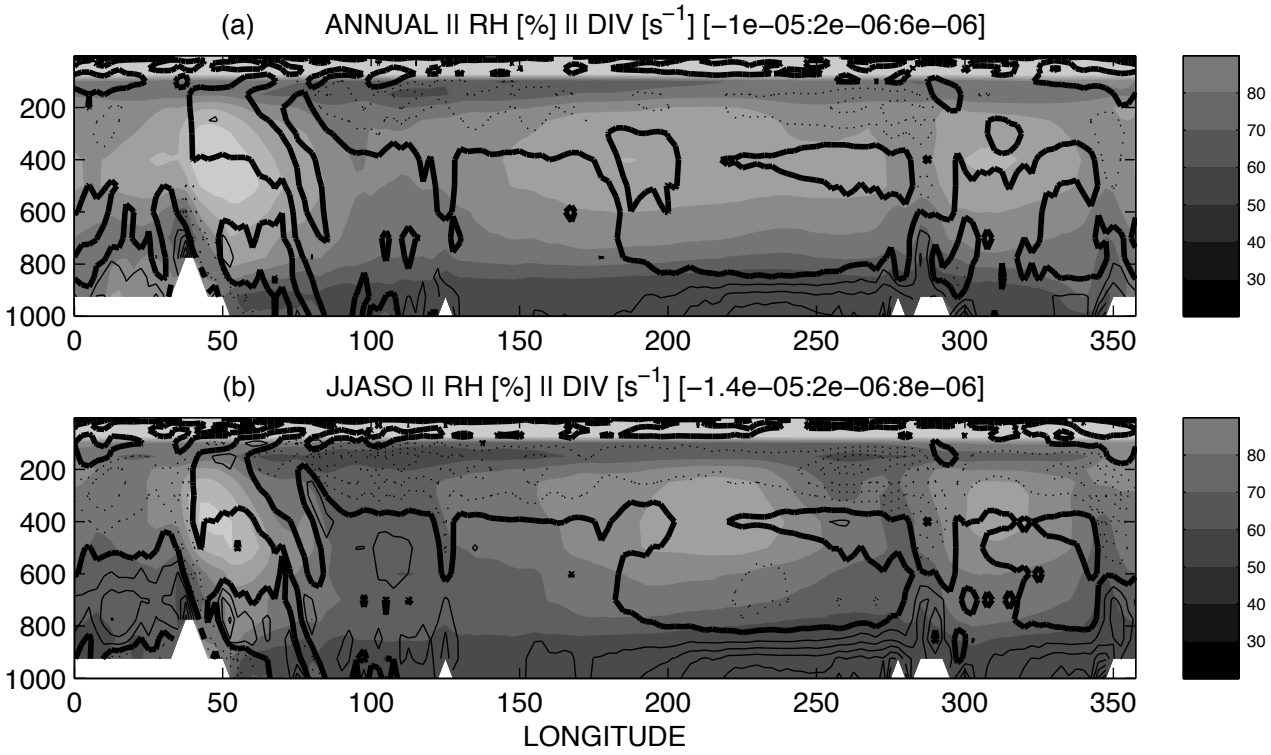


FIG. 1. Divergence and relative humidity climatologies from ERA40 re-analysis, averaged from 7.5$^o$N to 10$^o$N. The divergence is contoured, with solid contours denoting convergence, dashed contours divergence, and the thick contour the zero contour. Contour interval is 2x10$^{-6}$ s$^{-1}$. Relative humidity is shaded, with land areas solid white. (a) Annual mean and (b) mean for the months of June-October.

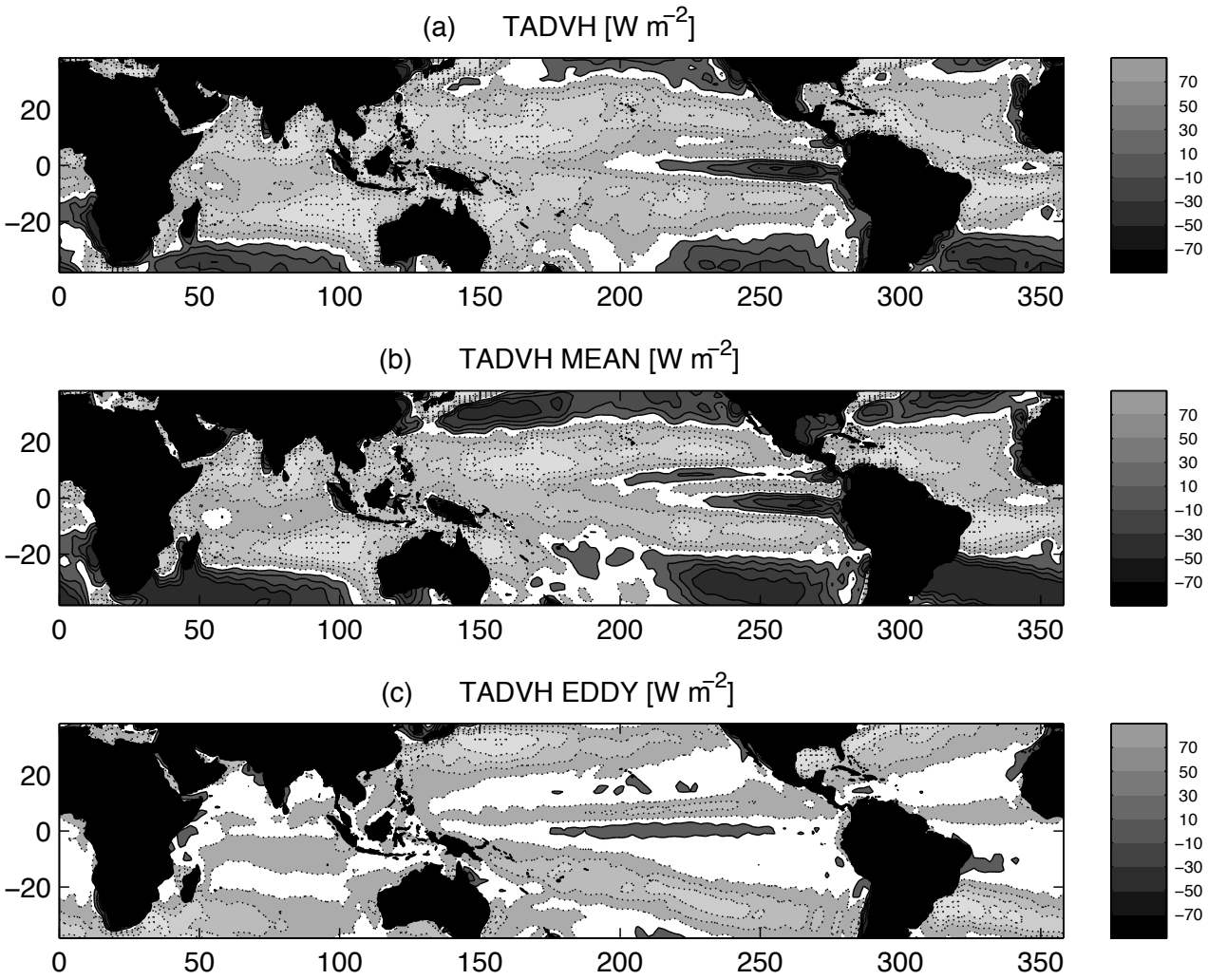


FIG. 2. Advective terms in the frozen moist static energy budget (3), re-gridded to a T63 regular Gaussian grid. (a) TADVH, (b) MADVH and (c) EADVH. Contour interval 20 W m$^{-2}$, with values less than -10 W m$^{-2}$ shaded lightly, and values greater than 10 W m$^{-2}$ shaded darkly.

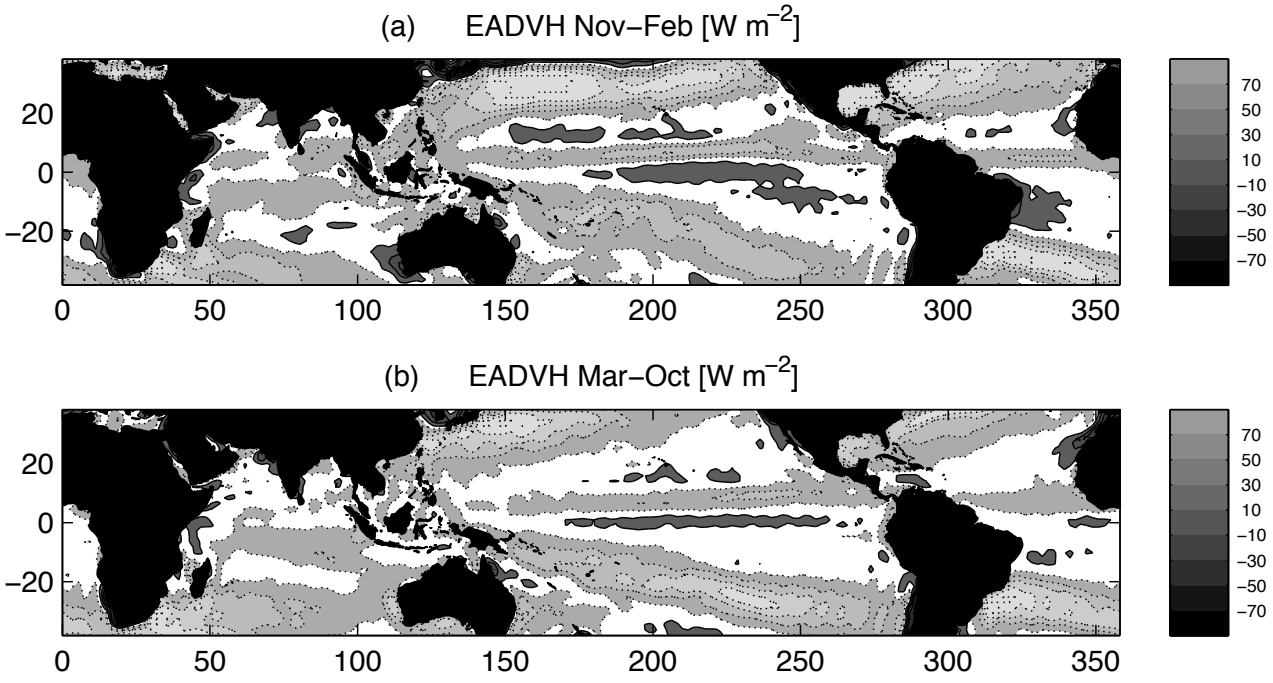


FIG. 3. Seasonal variation in EADVH. (a) EADVH averaged from November-February and (b) EADVH averaged from March-October. Shading and contours as in Fig. 2.

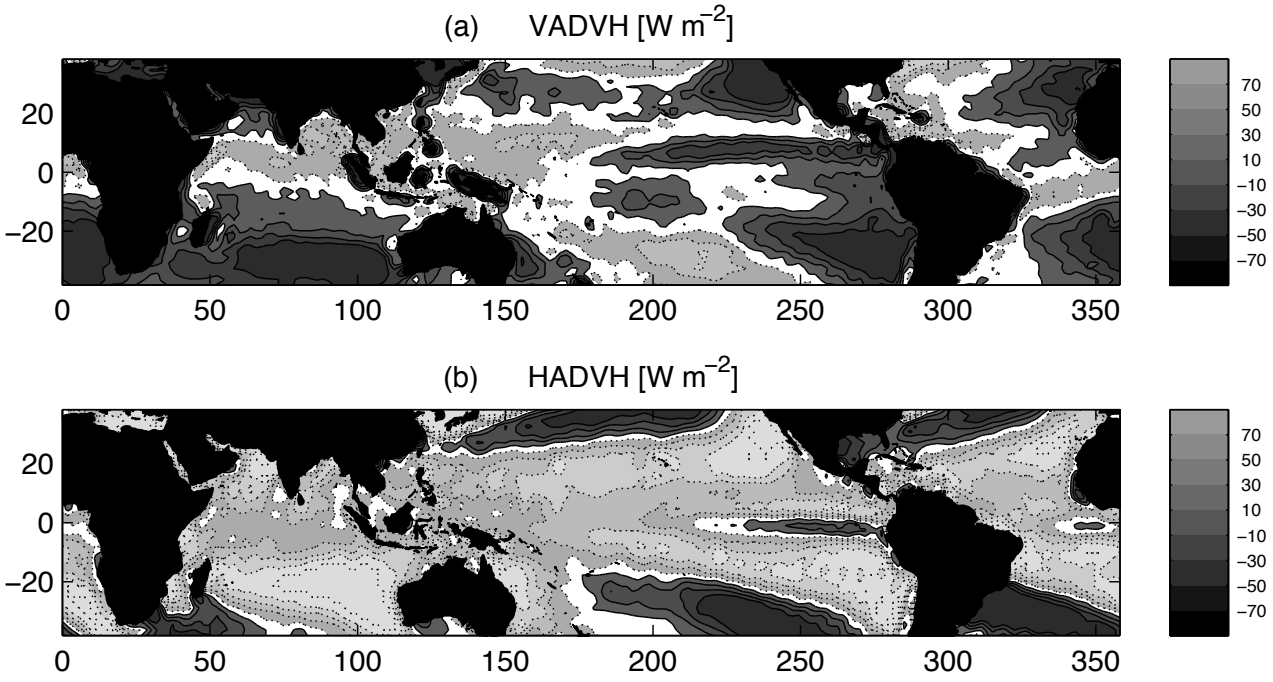


FIG. 4. As in 2 for the VADVH and HADVH terms in (4).

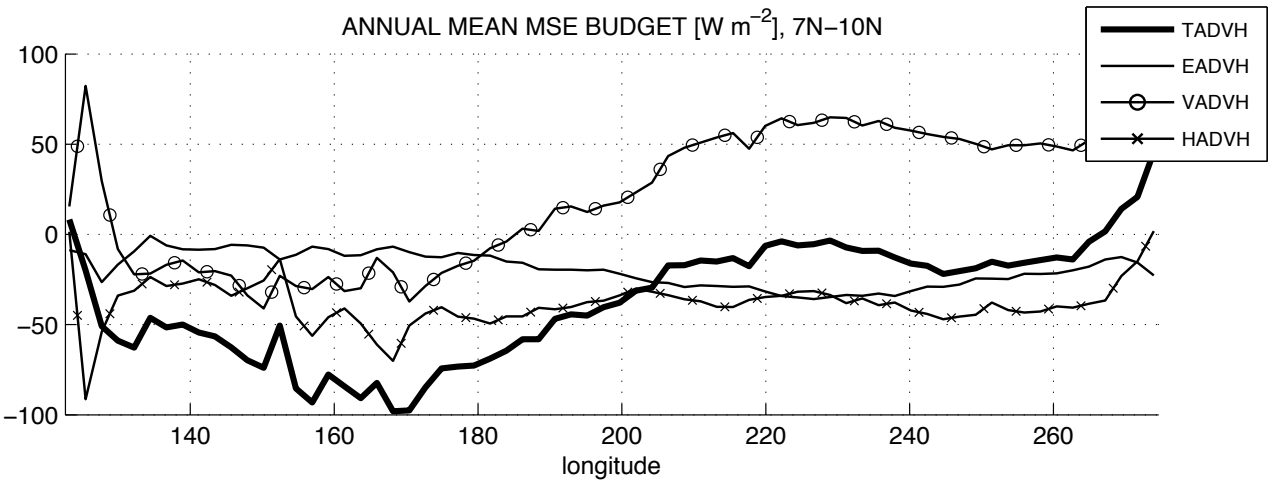


FIG. 5. Frozen moist static energy budget terms averaged between 7$^o$N and 10$^o$N, from the western to eastern Pacific (120E to 280E). The thick line is TADVH, thin line is EADVH, thin line with circles is VADVH and thin line with x's is HADVH.

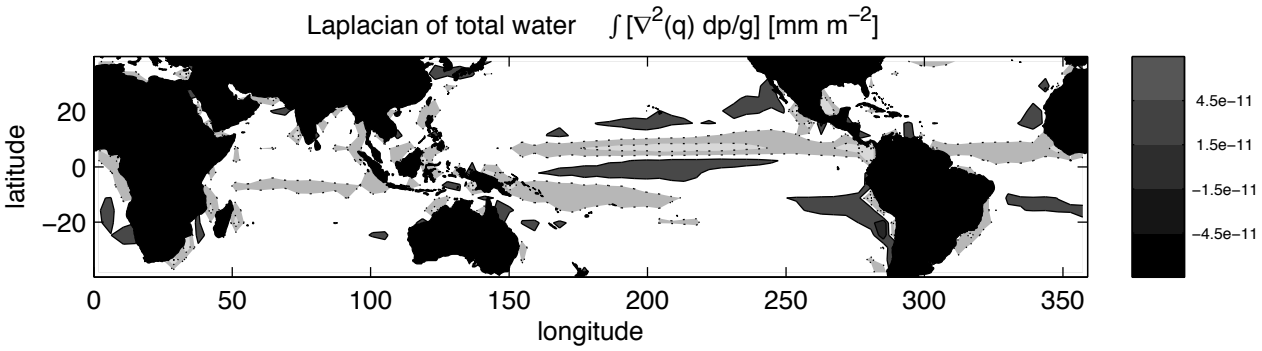


FIG. 6. Laplacian of mean precipitable water, block averaged into 4x4 blocks (approximately $4.5^o$ by $4.5^o$). Contour interval $3\text{x}10^{-11}$ mm $\text{m}^{-2}$, with values less than $-1.5\text{x}10^{-11}$ mm $\text{m}^{-2}$ shaded lightly, and values greater than $1.5\text{x}10^{-11}$ mm $\text{m}^{-2}$ shaded darkly.

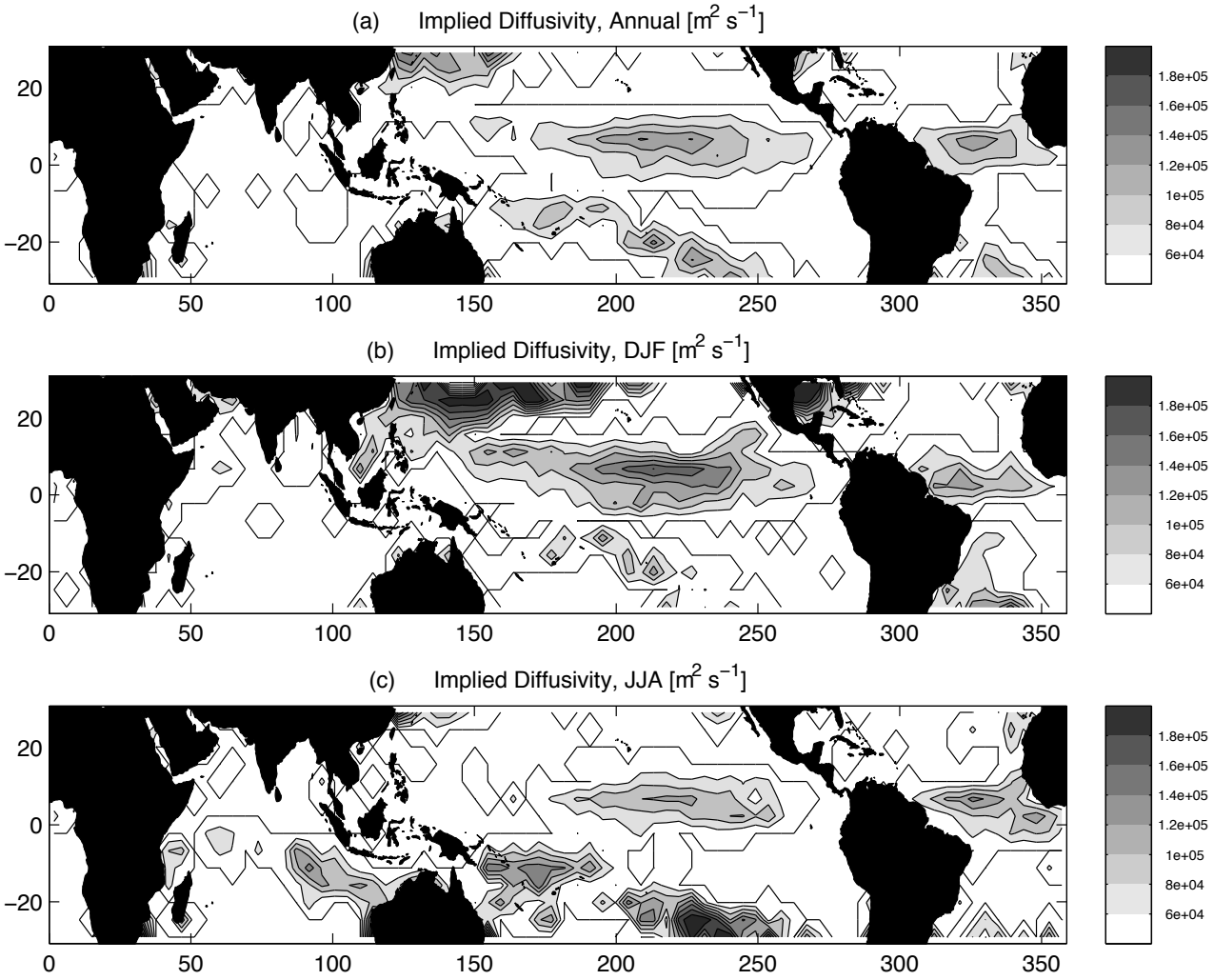


FIG. 7. Implied diffusivity, computed by regressing time series of the Laplacian of precipitable water onto EADVH. Block averaged into 4x4 blocks (approximately $4.5^o$ by $4.5^o$). Contour interval 2x$10^4$ m$^2$ s$^{-1}$.

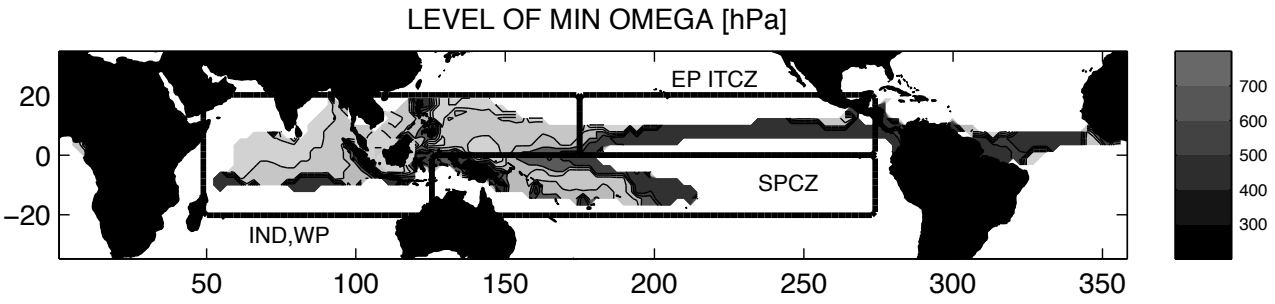


FIG. 8. Level of minimum time-mean $\overline{\omega}$ in all convecting grid boxes (defined to be those grid boxes with monthly mean precipitation larger than 6 mm day$^{-1}$), block averaged into 2x2 blocks. Contour interval 100 hPa. The solid lines denote the regions defined as "east Pacific ITCZ," "west Pacific-Indian" and "SPCZ" in Fig. 9.

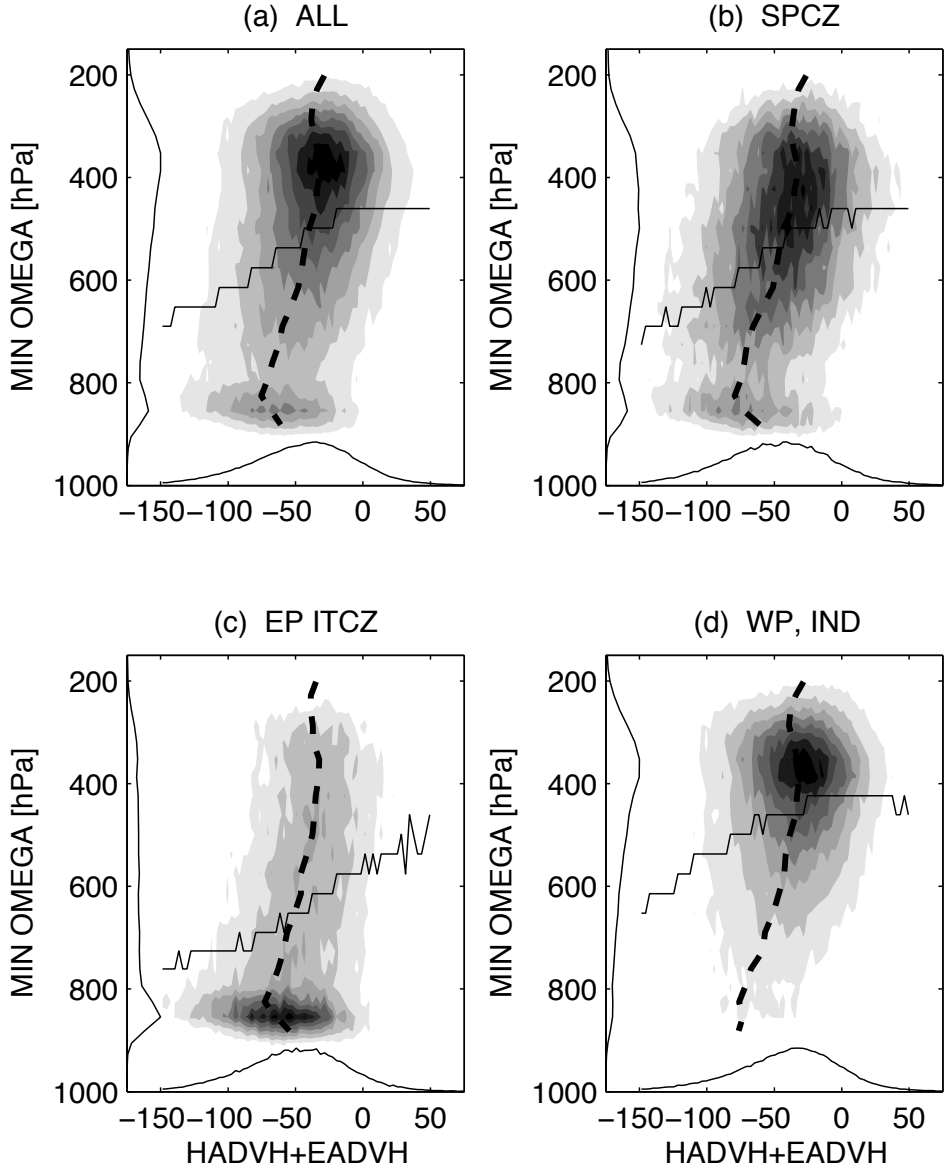


FIG. 9. Joint probability distribution functions of the sum of the HADVH and EADVH terms versus level of minimum $\omega$ (shading, with darker shading indicating more density). The marginal probability distribution functions are shown along each axis as solid lines. Starting from 2x2 block averaged monthly mean data, all ocean points between 20S and 20N with precipitation greater than 6 mm day$^{-1}$ were included. The mean HADVH+EADVH (level of minimum $\omega$) in each minimum $\omega$ (HADVH+EADVH) bin is shown with a dashed (solid) line. (a) All points in the Pacific and Indian Oceans, (b) only points in SPCZ, (c) only points in the east Pacific ITCZ, and (d) only points in the west Pacific and Indian Ocean.

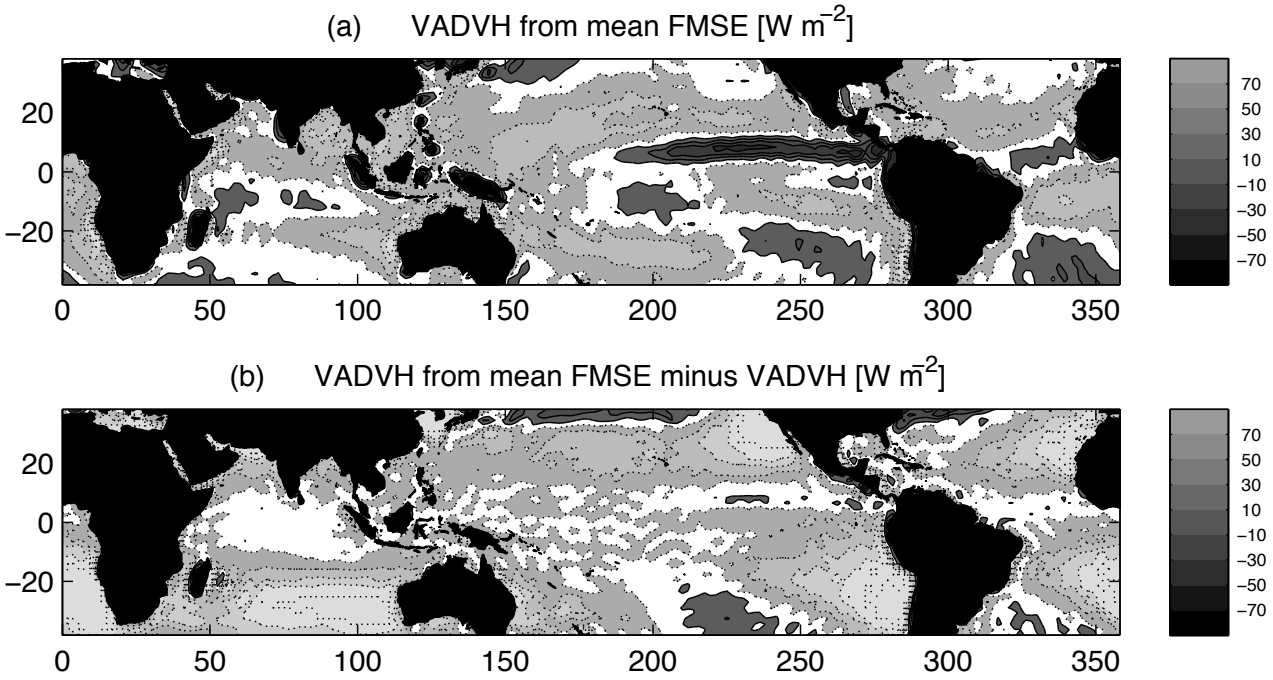


FIG. 10. (a) VADVH re-gridded to a T63 regular Gaussian grid, computed using the monthly mean FMSE profile over all convecting grid boxes from 20S-20N (defined to be those grid boxes with monthly-mean precipitation larger than 6 mm day$^{-1}$) and the spatially varying mass corrected horizontal winds. Contours and shading as in Fig. 2. (b) The difference between (a) and VADVH.

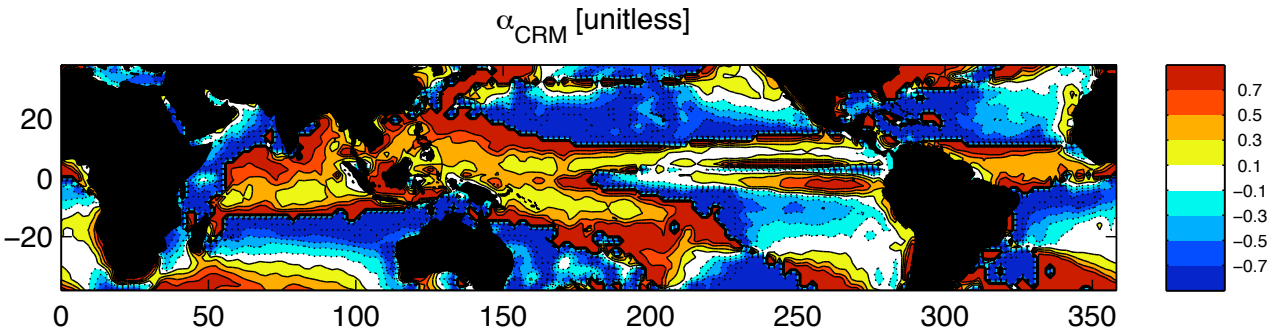


FIG. 11. $\alpha_{CRM}$ as defined in (5), re-gridded to a T63 regular Gaussian grid. Contour interval 0.2, with positive contours drawn as solid lines and negative contours dashed. The zero contour is omitted.